Electronic structure of yttrium aluminum garnet ($Y_3Al_5O_{12}$)

Yong-Nian Xu and W. Y. Ching
Department of Physics, University of Missouri-Kansas City, Kansas City, Missouri 64110
(Received 9 November 1998)

The electronic structure of yttrium aluminum garnet ($Y_3Al_5O_{12}$) is studied by means of first-principles local-density calculations. Results on band structure, density of states, partial density of states, effective charges, bond order, charge-density distributions, equilibrium lattice constant, bulk modulus, and pressure coefficient as well as the pressure dependence of the band gap are presented. The calculated results are in good agreement with experimental data. The differences in chemical bonding for Al ions at the octahedral and tetrahedral sites are clearly delineated and their implications discussed. [S0163-1829(99)03316-0]

I. INTRODUCTION

Yttrium aluminum garnet ($Y_3Al_5O_{12}$), or YAG, is the most important solid-state laser host material. Nd:YAG laser has been widely used in commercial, medical, military, and industrial applications since its discovery in 1964.[1] Apart from the ideal spectroscopic properties of the rare-earth ions in YAG crystal, its low-thermal expansion, high-optical transparency, low-acoustic loss, high threshold for optical damage, hardness, and general stability against chemical and mechanical changes all contribute to its success as the most widely used laser material.[2] It is also known that YAG is one of the most creep resistant oxide and therefore, has important applications in high-temperature ceramic composites.[3,4] YAG is frequently seen as the precipitated phase at the internal grain boundaries of alumina oxides or at the surface or interfaces of Al-containing metals. It is therefore surprising that there have been no fundamental studies on the electronic structure of the YAG crystal. The band structure and the chemical bonding in YAG is therefore unknown although optical and vibrational properties of YAG crystal have been extensively studied experimentally.[5–9] The refractive index and the elastic properties of YAG have also been investigated by a variety of experimental techniques.[10–13] The lack of reliable band-structure information on YAG made the interpretation of the optical data quite difficult. The main reason for the lack of theoretical investigations on YAG crystal is its enormously complicated crystal structure (to be discussed below) which renders detailed *ab initio* quantum-mechanical calculation computationally too demanding. With the rapid advance of computing technology and methodology in the last two decades, it is now possible to study the electronic structures for complex crystals such as YAG.

In this paper, we present the results of a detailed calculation of the ground-state electronic properties of the YAG crystal. We used the *ab initio* orthogonalized linear combinations of atomic orbitals (OLCAO) method[14] within the local-density approximation (LDA) of the density-functional theory.[15] The OLCAO-LDA method is noted for its efficiency and accuracy especially for systems with complex structures, and has been applied to other related crystals such as α-Al_2O_3 (Refs. 16 and 17) and Y_2O_3.[18] The O vacancy[19] and the Y-substitutional impurity in α-Al_2O_3 (Ref. 20) were also investigated using this method and a supercell approach. The method has been well described before and will not be repeated. In the present calculation, a full basis expansion consisting of atomic orbitals of Y (core orbitals $+5s,6s,4p,5p,6p,4d,5d$), Al (core orbitals $+3s,4s,3p,4p,3d$), and O ($1s$ core $+2s,3s,2p,3p$) were used. The semicore Y-$4p$ state was treated as a valence state since its orbital energy is only slightly lower than the O-$2s$ state. The crystal potential and charge density were represented by a sum of atom-centered functions consisting of gaussians. Wigner interpolation formula was used for correlation correction and four special **k** points in the irreducible portion of the Brillouin zone (BZ) were used for self-consistent iterations. The potential converges in about 20 iterations. The total energy of the crystal was calculated according to the usual LDA formalism.[14] The density of states (DOS) and its decomposition into atom- and orbital-resolved partial DOS (PDOS) were calculated based on the Mulliken scheme[21] using the wave functions obtained at the 14 *ab initio* **k** points within the BZ. The effective charges and the bond order (also called overlap population) were obtained by a separate minimal basis calculation.

In the next section, we discuss the crystal structure of YAG in some detail. In Sec. III, the results of the bulk properties are presented and discussed. This is followed by the discussion on the electronic structures in Sec. IV. The last section is for a brief conclusion and some thoughts on future work.

II. CRYSTAL STRUCTURE

The cubic unit cell of a general garnet compound $A_3B'_2B''_3O_{12}$ contains eight formula units, where A,B',B'' are metal ions occupying different symmetry sites.[22] The crystal structure of YAG is sketched in Fig. 1. It has a bcc structure (space group Ia3d or O_h^{10}) with 160 (80) atoms in the cubic (primitive) cell. The Y ions (A atom) occupy the 24(c) sites and each are dodecahedroally coordinated to eight O. The O atoms occupy the 96(h) sites whose exact locations depend on three structural parameters x, y, and z and are different for different garnet oxides. There are two different sites for Al, Al_{oct} (B' atom) occupy the 16(a) site with an octahedral point symmetry (C_{3i}) and Al_{tet} (B'') atoms occupy the 24(d) sites with a tetrahedral point symmetry (S_4). The garnet

 ©1999 The American Physical Society

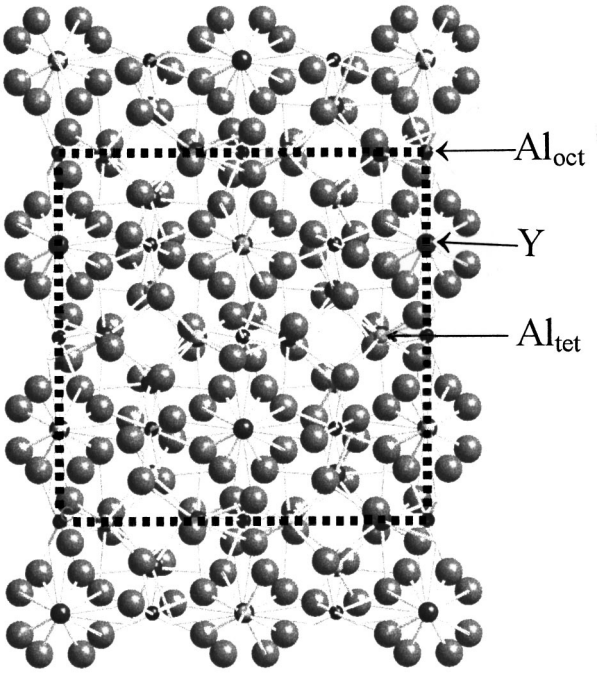

FIG. 1. Crystal structure of YAG viewed along the [001] direction. The large balls are O, the intermediate balls are Y, the small balls are Al. Octahedrally bonded Al_{oct} and tetrahedrally bonded Al_{tet} are as indicated. The dotted lines represent the cubic cell boundary. Al_{oct} are at the corner, the edge center, the face center, and the quarter face center positions.

structure can be viewed as interconnected octahedraons, tetrahedrons, and dodecahedrons with shared O atoms at the corners.[22] (Each oxygen is a member of two dodecahedra, one octahedron, and one tetrahedron.)

There have been several structural measurements on YAG with results quite close to each other.[23–27] We have used the structure determined by Euler and Bruce[25] in the present calculation. The lattice constant is 12.000 Å. Cations are at fixed positions while the O sublattice is slightly distorted depending on the internal parameters. For the YAG crystal, the O parameters are $x=-0.0306$, $y=0.0512$, and $z=0.1500$. It should be noted that the Y-O separations are 2.303 and 2.432 Å, larger than in Y_2O_3 (2.288 Å); and the Al-O separations are 1.937 and 1.761 Å, slightly smaller than 1.969 and 1.857 Å in α-Al_2O_3. The O-O separations range from 2.658 to 2.917 Å.

III. BULK PROPERTIES

The total energy (TE) of the YAG crystal was calculated as a function of crystal volume with the internal parameters fixed. The results are shown in Fig. 2. Our calculation predicts an equilibrium lattice constant of 11.904 Å, which differs from the measured one by less than 1.0%. The TE curve in Fig. 2 was fitted to three different equations of states (EOS): a fourth order polynomial, the Murnaghan EOS (Ref. 28) and the Birch-Murnaghan EOS.[29] The results are quite close for B with a larger variation for the pressure coefficient B'. The fit using Mirnaghan EOS gives a bulk modulus of $B=220.7$ Gpa and a pressure coefficient of $B'=4.12$ (Table I). This is in excellent agreement with the value of $B=220.0$ Gpa of Hofmeister and Campbell[11] obtained from an empirical formula and the measured infrared vibrational frequencies of YAG. On the other hand, Stoddart *et al.* obtained a room-temperature value of $B=189$ Gpa based on the room-temperature elastic constants using a combination of Brillouin scattering and refractive index measurements.[12] An earlier measurement by Alton and Barow[13] gave B value of 185.2 Gpa.

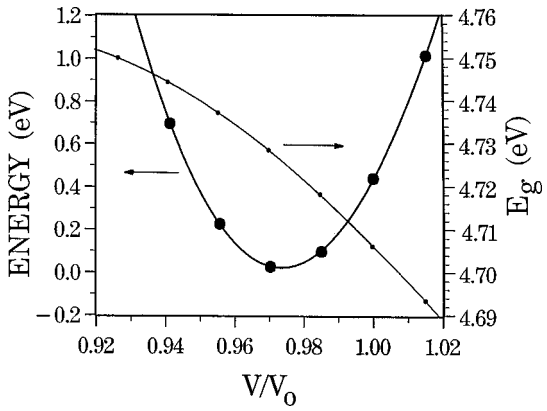

FIG. 2. Calculated total energy (left scale) and band gap E_g (right scale) vs V/V_0 in YAG. V_0 is the experimental equilibrium volume taken to be 864.000 Å^3 here.

Figure 2 also shows the volume dependence of the direct band gap *Eg* (to be discussed in the next section). From the slope of the E vs V/V_0 curve, the pressure at each volume can be obtained and hence the pressure dependence of the gap. The dependence of *Eg* on *P* near the calculated equilibrium volume is approximately linear with an initial slope of 0.025 eV/Gpa. This is to be compared with the value of 0.012 eV/Gpa in a similar calculation for Y_2O_3.[18] In Y_2O_3, the *Eg* vs V/V_0 curve is almost linear down to 10% reduction in volume. In YAG, the same curve shows a much less change in *Eg* as the volume is decreased, which results in a larger pressure dependence of the gap than in Y_2O_3. We are not aware of any experimental measurements related to the change of gap under pressure.

IV. ELECTRONIC STRUCTURE

Figure 3 shows the calculated band structure of YAG at the experimental lattice constant. The band gap of 4.71 eV is direct at Γ. This is 28% smaller than the experimental value

TABLE I. Calculated bulk modulus and pressure coefficient of YAG using different EOS's.

	B (Gpa)	B'
Fourth order polynomial	228.6	4.60
Murnaghan	220.7	4.12
Birch-Murnaghan	221.1	4.00
Experimental value	220.0[a]	
	185.2[b]	
	189.0[c]	

[a]Reference 11.
[b]Reference 12.
[c]Reference 13.

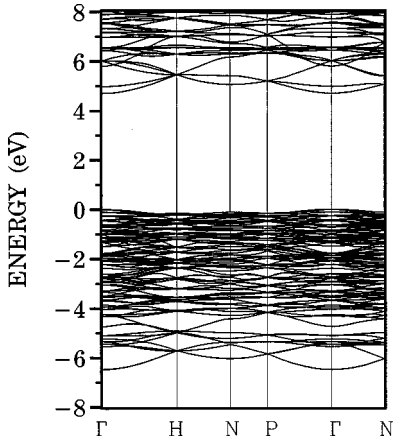

FIG. 3. Calculated band structures of YAG along the symmetry lines of the cubic BZ.

of 6.5 eV deduced from optical measurements.[6–9] Such an underestimation of the gap value is typical of the LDA calculations. The top of valence band (VB) is very flat, similar to all other Y- or Al-related oxides. It is interesting to note that the conduction-band (CB) edge at Γ in YAG consists of two rather well-separated bands while in α-Al_2O_3 (Ref. 17) and Y_2O_3,[18] there is only a single CB dipping down at Γ. This could be due to the presence of two nonequivalent cations in YAG and the specific symmetry of the crystal.

Figure 4 shows the total and atom-resolved partial density of states (DOS) in YAG. The sharp peaks near −20 eV are the semicore levels of Y-4p, which were treated as valence states in the present calculation. The O-2s levels are between −15 and −17.5 eV and the O-2p levels constitute the upper VB with a total width of about 6.5 eV. The same O-2p band has a width of 7.37 eV in α-Al_2O_3 and 3.41 eV in Y_2O_3. The PDOS of Y has a sharp peak at 6.5 eV in the CB and also show slight mixing with O-2p and O-2s in the VB region. At the bottom of the CB, Y has the largest component so the band gap in YAG is essentially determined by the Y-O interaction rather than the Al-O interaction. The calculated gap of YAG is smaller than that of α-Al_2O_3, which is consistent with the notion that α-Al_2O_3 is more ionic than Y_2O_3. This point is further supported by the effective charge calculations to be discussed below. The difference in the PDOS between Al_{oct} and Al_{tet} are quite obvious, especially in the 0 to −2.5 eV range in the VB and in the shape and locations of the peaks in the CB. As expected, the PDOS of oxygen are mostly in the VB with less prominent features in the CB.

The orbital resolved PDOS in the CB are shown in Fig. 5 (broadened by 1.0 eV). The $(s+d)$ component is for the even parity and the p component is for the odd parity of the angular momentum quantum number. Within the dipole approximation, orbital-resolved PDOS can be used to interpret the electron-loss near-edge spectroscopy (ELNES) which has become a very popular tool to investigate local chemical and structural environment of a particular ion.[30] So the $(s+d)$ and the p components of the Al-PDOS should mimic Al-$L_{2,3}$ edge and the Al-K edge, respectively, and the Y-$(s+d)$ PDOS should reproduce the Y-$L_{2,3}$ and Y-$M_{2,3}$ edges, while the O-p PDOS can be used to compare with the O-K edge. Such comparisons have been carried out recently with the

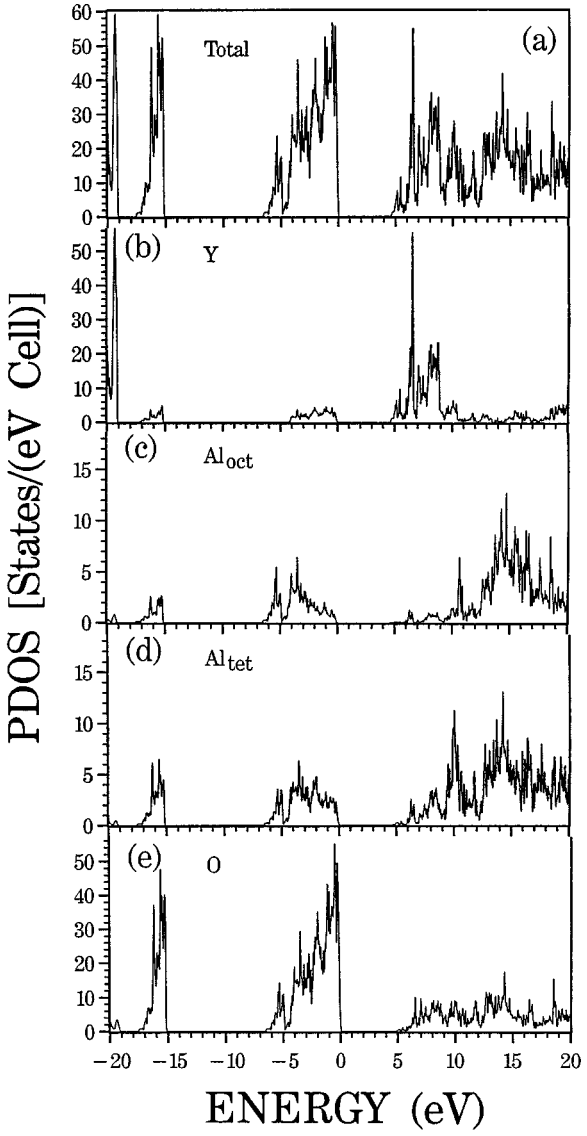

FIG. 4. Calculated total DOS and atom-resolved PDOS of YAG (a) Total; (b) Y; (c) Al_{oct}, (d) Al_{tet}; and (e) O.

measured ELNES data in YAG with satisfactory agreements.[31] It turns out that the differences between the Al_{oct} and Al_{tet} sites are essential for a proper interpretation of the experimental spectra. Below 11 eV, Al_{tet} has a much higher amplitude than Al_{oct}. This is particularly true for the p component of the Al PDOS, which mimic the Al-K edge.

Based on the *ab initio* wave functions obtained throughout the BZ and the Mulliken population scheme, the effective charges on each atom and the bond order between each pair of atoms in YAG were calculated as previously described.[18] A separate minimal basis calculation were carried out for this purpose since the Mulliken analysis scheme is more accurate with a minimal basis than with an extended basis. The results are listed in Table II together with the results from similar calculations for α-Al_2O_3 and Y_2O_3. The effective charge calculation indicates that among the three crystals, α-Al_2O_3 is the most ionic and Y_2O_3 the least ionic. Y ion has less charge transfer to O than Al, and the traditional viewpoint of treating both Al and Y as 3+ ions may be problematic. The bond order, also called the overlap

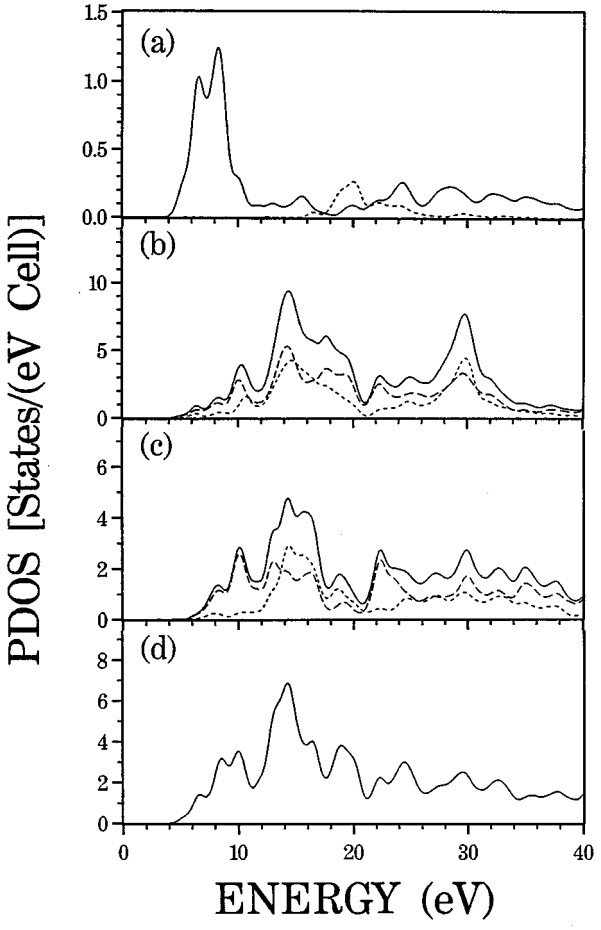

FIG. 5. Orbital resolved PDOS of the empty CB: (a) Y, solid line (dashed line) for the $s+d(p)$ component. (b) $(s+d)$ component of Al. Solid line for total, dotted line for Al_{oct}, and dashed line for Al_{tet}. (c) p component of Al. Solid line for total, dotted line for Al_{oct}, and dashed line for Al_{tet}. (d) O-p component.

population, is a simple qualitative measure of the strength of the bond between a pair of atoms α and β. The bond order between the second nearest-neighbor O-O and cation-cation pairs are also listed together with their interatomic separations. However, the bond order for Y-Y pairs are not included because they are negligibly small. It should be noted that the bond orders for ionic systems such as α-Al_2O_3, Y_2O_3, and YAG are much smaller than those in the more covalently bonded compounds such as Si_3N_4 or Si-Al-O-N.[32] Although the bond order scales roughly with the distances of separation, the bond order for Al_{tet}-O in YAG is relatively large compared to all other pairs. Given the fact that 60% of the Al sites are the Al_{tet} tetrahedral site, this large bond order

TABLE II. Calculated effective charge Q_α^* in α-Al_2O_3, Y_2O_3, and YAG crystals

	α-Al_2O_3	Y_2O_3	YAG
Al	1.890		1.843
			2.036
Y (excluding $4p$)		2.078	2.033
		2.097	
O	6.740	6.606	6.676

TABLE III. Calculated bond order $\rho_{\alpha,\beta}$ in α-Al_2O_3, Y_3O_3, and YAG crystals. Interatomic distances list in parenthesis (Å).

	α-Al_2O_3	Y_2O_3	YAG	
Al-O	0.105 (1.857)		Al_{oct}-O	0.096 (1.937)
	0.083 (1.969)		Al_{tet}-O	0.133 (1.761)
Y-O		0.098 (2.261)		0.075 (2.432)
		0.104 (2.249)		0.081 (2.303)
		0.092 (2.278)		
		0.087 (2.336)		
O-O	0.022 (2.524)	0.015 (2.659)		0.005 (2.865)
	0.019 (2.619)	0.014 (2.696)		0.004 (2.927)
	0.012 (2.725)	0.010 (2.818)		0.002 (3.168)
	0.008 (2.869)	0.007 (2.837)		
		0.006 (2.917)		
		0.007 (2.961)		
Al-Al	0.026 (2.649)			
	0.024 (2.792)			
Y-Al_{oct}				0.017 (3.354)
Y-Al_{tet}				0.041 (3.000)

provides the evidence that the overall good mechanical properties of the YAG crystal is due to the presence of the tetrahedral Al sites. It is also noted that the bond order between Y and Al_{tet} in YAG at a separation of 3.0 Å is 0.041, larger than that between Al-Al and O-O pairs in α-Al_2O_3 with smaller separations. This could mean that Al_{tet} at the tetrahedral site may actually interact with a nearby Y atom in spite of the fact that there are both cations (Table III).

Figures 6(b) and 7(b) display the valence charge-density distribution in YAG crystal on two (001) planes with $z=0.0$ and 0.6, respectively. The first plane contains all the cations and the second one contains only the O anions. Figures 6(a) and 7(a) show the positions of various ions in these planes or slightly off these planes. Figures 6(c) and 7(c) show the difference of the crystal charge and that of a superposition of neutral atomic charges on the same plane. Several observations can be made from these distributions. (1) The charge distributions around the ions including O are nonspherical, indicating a considerable amount of charge redistribution. (2) The distribution of charges at Al_{oct} and Al_{tet} are quite different reflecting the inference of the local symmetry. (3) The Y atom has a concentric ring of near zero charge due to the coincidence of the nodes of the Y-5s and Y-4d atomic orbitals in the basis function.[18] The Y-4d wave function is actually quite extended, which facilitates its bonding with other ions. (4) From the contour lines of Fig. 6, there is some evidence of interaction between Y and Al_{tet} in spite of the distance of separation of 3 Å. (5) The majority of the charge transfer occur at the outer ring of the Y ion as is evident in Figs. 6(c) and 7(c).

V. CONCLUSIONS

The electronic structure and properties of the YAG crystal were calculated. Good agreements with experimental data in terms of the equilibrium lattice constant and the bulk modulus are obtained. The calculated orbital-resolved PDOS also show good agreement with the recently measured ELNES

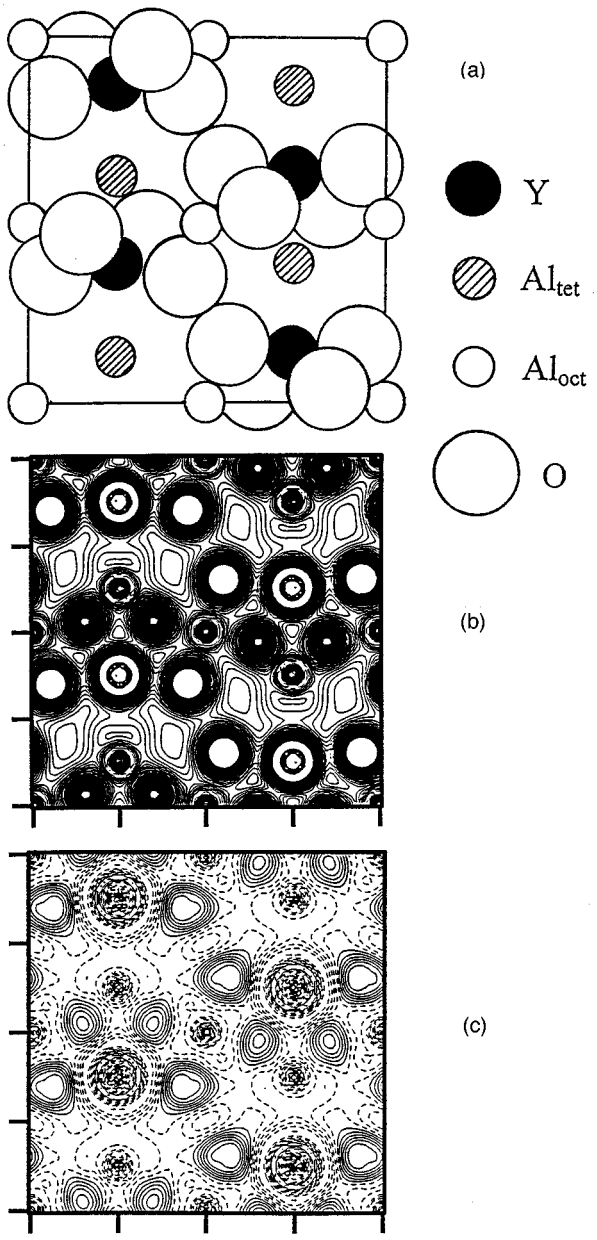

FIG. 6. (a) Atomic configuration in the (001) plane with $z = 0.0$ containing all cations. The O ions are slightly above or below the plane. (b) Valence charge-density contours in the same plane. The contour lines range from 0.00 to 0.25 electrons/(a.u.)^3 in intervals of 0.005. (c) Difference between crystal valence charge density and a superposition of atomic valence charges. Solid (dashed) lines for the positive (negative) contours. Contour lines range from -0.25 to 0.25 electrons/(a.u.)^3 in intervals of 0.005.

spectra. The calculation shows different PDOS for Al_{oct} and Al_{tet} because of the different local symmetry. It is pointed out that Al_{tet} form stronger bonds and may interact with the Y atoms thus contribute to the unique properties of the YAG crystal.

With the electronic structure of YAG crystal well understood, it is natural that future investigations should include the calculations of optical properties of the YAG as well as impurity states such as Cr^{3+}, Cr^{4+}, and Nd^{3+} in YAG. It is also desirable that the other two remaining Y-Al-O compounds, $YAlO_3$ (YAP) and $Y_4Al_2O_9$ (YAM), with different crystal structures and local bonding be studied in the same fashion. Such work are currently in progress and will be reported at a later time.

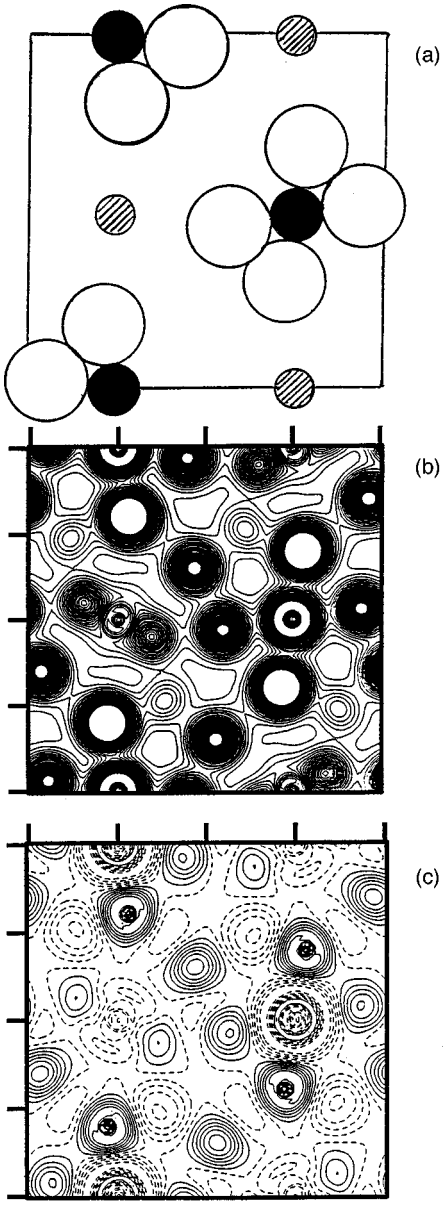

FIG. 7. Same as Fig. 6 for a (001) plane with $z = 0.60$ containing O ions with the Y ions slightly off the plane.

ACKNOWLEDGMENT

This work was supported by the U.S. Department of Energy under Grant No. DE-FG02-84DR45170.

[1] J. E. Geustic, H. M. Marcos, and L. G. Van Uitert, Appl. Phys. Lett. **4**, 182 (1964).
[2] See, for example, R. C. Powell, *Physics of Solid State Laser Materials* (AIP, New York, 1998).
[3] J. D. French, J. Zhao, M. P. Harmer, H. M. Chan, and G. A. Miller, J. Am. Ceram. Soc. **77**, 2857 (1994).
[4] S. Deng, J. Mater Sci. **31**, 6077 (1996).
[5] J. P. Hurrell, S. P. S. Porto, I. F. Chang, S. S. Mitra, and R. P. Bauman, Phys. Rev. **173**, 851 (1968).
[6] G. A. Slack, D. W. Oliver, R. M. Chrenko, and S. Roberts, Phys. Rev. **177**, 1308 (1969).
[7] Y. Zhan and P. D. Coleman, Appl. Opt. **23**, 548 (1984).
[8] T. Tomiki, F. Fukudome, M. Kaminao, M. Fujisawa, Y. Tanahara, and T. Futemma, J. Phys. Soc. Jpn. **54**, 4429 (1988); **58**, 1801 (1989).
[9] T. Tomiki, Y. Ganaha, T. Shikenbrau, T. Futemma, M. Yuri, Y. Aiura, H. Fukutani, H. Kato, J. Tamashiro, T. Miyahara, and A. Yonesu, J. Phys. Soc. Jpn. **62**, 1388 (1993); **65**, 1106 (1996).
[10] R. D. Shannon *et al.*, J. Appl. Phys. **67**, 3798 (1990).
[11] A. M. Hofmeiser and K. R. Campbell, J. Appl. Phys. **72**, 638 (1992).
[12] P. R. Stoddart, P. E. Ngoepe, P. M. Mjwara, J. D. Comins, and G. A. Saunders, J. Appl. Phys. **73**, 7298 (1993).
[13] W. J. Alton and A. J. Barow, J. Appl. Phys. **32**, 1172 (1967).
[14] W. Y. Ching, J. Am. Ceram. Soc. **71**, 3135 (1990).
[15] P. Hohenberg and W. Kohn, Phys. Rev. **136**, B864 (1964); W. Kohn and L. J. Sham, *ibid.* **140**, A1133 (1965).
[16] Y.-N. Xu and W. Y. Ching, Phys. Rev. B **43**, 4461 (1991).
[17] W. Y. Ching and Y.-N. Xu, J. Am. Ceram. Soc. **77**, 404 (1994).
[18] Y.-N. Xu, Z.-Q. Gu, and W. Y. Ching, Phys. Rev. B **56**, 14 993 (1997).
[19] Y.-N. Xu, Z.-Q. Gu, X.-F. Zhong, and W. Y. Ching, Phys. Rev. B **56**, 7277 (1997).
[20] W. Y. Ching, Y.-N. Xu, and M. Rühle, J. Am. Ceram. Soc. **80**, 3199 (1997).
[21] R. S. Mulliken, J. Chem. Phys. **23**, 1833 (1955).
[22] F. S. Galasso, *Structure and Properties of Inorganic Solids* (Pergamon, New York, 1970), p. 244.
[23] H. S. Yoder and M. L. Keith, Geol. Soc. Am. Bull. **61**, 1516 (1950).
[24] A. Emiraliev *et al.*, Kristallografiya **21**, 211 (1976) [Sov. Phys. Crystallogr. **21**, 112 (1976)].
[25] F. Euler and J. A. Bruce, Acta Crystallogr. **19**, 971 (1965).
[26] E. Price, Acta Crystallogr., Sect. B: Struct. Crystallogr. Cryst. Chem. **24**, 1968 (1982).
[27] T. S. Chernaya *et al.*, Kristallografiya **34**, 1292 (1989) [Sov. Phys. Crystallogr. **34**, 778 (1984)].
[28] F. D. Murnagan, Proc. Natl. Acad. Sci. USA **30**, 244 (1944).
[29] F. Birch, J. Geophys. Res. **83**, 1257 (1957).
[30] R. F. Egerton, *Electron Energy Loss Spectroscopy in the Electron Microscopy* (Plenum, New York, 1993).
[31] M. A. Gülgün, W. Y. Ching, Y.-N. Xu, and M. Rühle (unpublished).
[32] W. Y. Ching, M.-Z. Huang, and Shang-Di Mo (unpublished).